DTU Library

Probability of Failure due to Electrochemical Migration on Surface Mount Capacitor under Electrolyte Condition with same Contamination and Conductivity Level

Bahrebar, Sajjad; Ambat, Rajan

Link back to DTU Orbit

Probability of Failure due to Electrochemical Migration on Surface Mount Capacitor under Electrolyte Condition with same Contamination and Conductivity Level

Sajjad Bahrebar*, Rajan Ambat

Center for Electronic Corrosion, Section of Materials and Surface Engineering, Department of Civil and Mechanical Engineering,
Technical University of Denmark, 2800 Lyngby, Denmark
Email: sajbahr@dtu.dk

Abstract— The effect of three common no-clean solder flux residues (adipic acid, glutaric acid, and succinic acid) as contamination types at three low levels (same concentrations) as well as in the same conductivity value in comparison with sodium chloride (NaCl) on time to failure (TTF) due to electrochemical migration (ECM) on the surface mount capacitors (SMCs) were investigated. The relation between TTF and leakage current (LC), conductivity, number of failures, as well as the probability of failure (PoF) using applicable probabilistic distributions in various conditions combined with diverse contamination types/levels and voltage based on many replications were studied.

Keywords— electrochemical migration; time to failure; probability of failure; surface mount capacitor; contamination type and level; conductivity.

I. INTRODUCTION

Contamination typically found inside electronic devices originates from both the printed circuit board assembly (PCBA) manufacturing process (intrinsic contamination) and the atmospheric particles (extrinsic contamination) [1], [2]. However, process related intrinsic contamination on the PCBA surface is most important in almost all cases, as extrinsic contamination entry to the PCBA surface is avoided by proper packaging [3]. Therefore, major hygroscopic residues causing problems on the PCBA surface arise from the solder flux residue resulting from the manufacturing process [4]. Certain amounts of residues remaining on a PCBA surface due to its hygroscopic nature attract humidity from the surrounding environment and build up water layer, act as corrosion accelerated factors, and contribute to deterioration in the electronic device's functionality [4], [5]. The soldering process, especially wave soldering because of the use of liquid flux by spraying process, introduces ionic residues on the PCBA surface during the manufacturing process, which along with other factors, affects the corrosion failures related to humidity on the PCB surface [6], [7]. Most of the no-clean flux systems today are based on weak organic acid (WOA) activators [8]. Typically, these acids can be adipic, succinic, and glutaric, to name a few, which are hygroscopic similar to sodium chloride (NaCl). Due to hygroscopic properties, most of the contaminations on PCBAs are also highly soluble in water, which can uptake humidity and enrich formation of a layer with some electrical conductivity on the PCB surfaces, causing different failures [9]. Besides, both WOAs solubility and WOAs strength will define the conductivity of the water layer made on the PCBA. The high conductivity of the water layer usually leads to high leak current between biased points on PCBA, which in most cases leads to increased corrosion failures. The WOAs solubility determined how much residue that can dissolve at a temperature, and WOAs strength determines the dissociation ability of the acids (determined by the pKa values) [10]. The PCBA contaminations are due to their hygroscopic feature mostly connected to the flux residues from the soldering process assisting water layer increase, and possible corrosion creation [11], [12]. The formation of water film, along with applying potential bias, results in a leak current between opposite biased points on the PCBA surface and the electrochemical migration (ECM) phenomenon as one of the most common electrochemical failure mechanisms in PCBAs [13], [14]. The importance of the ECM refers to migration of metal ions between two opposite points of electrodes (anode and cathode on a component or between components) through the conductive electrolyte (water layer formation on the surface at various climatic conditions) under the effect of the electric field due to applying the potential bias between two opposite point [14], [15]. Subsequently, it can affect product performance and lead to severe deterioration and corrosion of electronic devices.

Previous works showed that most of the studies carried out are in high contamination levels, where there is a high amount of flux residue in low water layer thickness, meaning that the water layer will have very high concentrations of acid on surface insulation resistance (SIR) PCBs [16], [17], [18], [19]. Many of these acids also act as corrosion inhibitors due to the possibility of adsorbing to the metal surfaces because of the carboxyl group [20], [21]; therefore, it is interesting to understand how low concentrations of these contaminations, as well as same conductivity, will influence time to failure (TTF) due to ECM. Besides, based on some studies that showed the probability of ECM does not follow the linear trend by increasing voltage and contamination levels [22], [23]; this study tried to find the appropriate probabilistic distribution of the TTF trend utilizing 20 replications for each condition to find the probability of failure (PoF). Accordingly,

two different experiments using droplet tests have been performed at various conditions to investigate the influence of voltage at two levels of 5 and 10 V, as well as four contamination types (three WOAs and NaCl) at similar contamination levels (1, 10, and 20 $\mu g/cm^2$) and the equivalent conductivity level (~203 $\mu s/cm$) based on the TTF values in the SMC component.

II. MATERIALS AND METHODS

A. Surface mount capacitor

Surface mount capacitor (SMC) is one of the important components that commonly use in PCBA surface mount technology. All the experiments were performed on the SMCs with electronic industries association (EIA) code 0805 housing size of a multilayer ceramic chip capacitor with 10 nF capacitance, 50 V voltage range, and electrode terminals of tin [9], [24]. For statistical and probabilistically analysis, 20 SMCs were utilized for each condition combined with various voltage, contamination types and levels, Fig. 1 displays the SMC used for this study with dimensions of 2 mm length, 1.2 mm width, and 0.45 mm height.
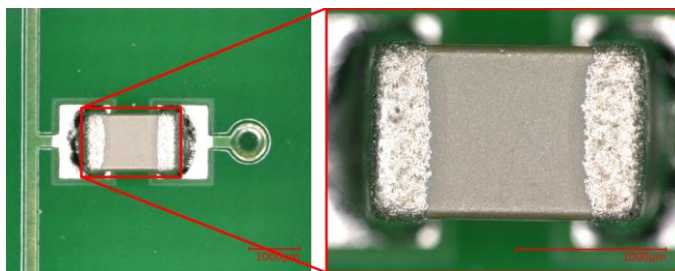

Fig. 1. View of single SMC consists of tin (Sn) in end terminals.

B. Droplet test and experimental data conditions

Droplet test is an accelerated lifetime test to assess the TTF on PCBA components [25]. For this investigation, a droplet of 2 μl constant volume of four different contamination types, including adipic acid, glutaric acid, succinic acid, and NaCl solution in water, is placed on top of each SMC surface.

Three concentrations of adipic acid, glutaric acid, and succinic acid from WOAs, as well as NaCl electrolyte solutions, were used for testing, including; 0.0013 g/l, 0.013

g/l, and 0.026 g/l. The steady amount of solutions over a constant area for all the experiments of 0.24 cm^2 and pitch distance of 1400μm was used to fix the contamination levels in $\mu g/cm^2$ unit.

Using a micropipette, the solution droplet is positioned between two opposite electrodes to connect the anode and cathode under two different DC voltages. This condition creates an aggressive situation, which causes increasing high leakage current (LC) followed by dendrite formation and ECM on the component surface. The BioLogic VSP potentiostat is used to apply 5, and 10 DC voltages to the SMCs and measure leak current. Fig. 2 displays the droplet test on an SMC in connection with a potentiostat to measure leak current under a digital microscope.

Fig. 2. Droplet test on an SMC in connects to potentiostat under a digital microscope.

In this study, two different experiments have been performed to investigate the influence of similar contamination levels and the same conductivity level on TTF based on many replications on the SMCs. Table I presents the details of all contamination types in similar contamination levels, which are used [26], [27]. In the first experimental setup, three levels of each contamination at two voltage levels provide six diverse conditions. It means in each contamination type, six conditions with twenty replications (4 contamination types, each at 6 conditions, every condition with 20 replications) have been analysed, and 240 runs have been delivered at 7200 min.

TABLE I.

OVERVIEW OF THE FIRST EXPERIMENTAL SETUP USING SIMILAR CONTAMINATION LEVELS OR THE SAME AMOUNT OF ACID IN WATER AS ELECTROLYTE SOLUTIONS ON SMC SURFACES .

Contaminations	pKa1	pKa2	Solubility in water at 25 °C (g/l)	Conductivity (µs/cm) at:			Amount of contaminations in 100 ml D-water equivalent in order to have the same contamination level at:			Molecular weight (g/mol)	Concentration (moles/Liter) at:		
				1 µg/cm²	10 µg/cm²	20 µg/cm²	1 µg/cm²	10 µg/cm²	20 µg/cm²		1 µg/cm²	10 µg/cm²	20 µg/cm²
Adipic	4.44	5.43	24	14	64	92	0.0013g	0.013g	0.026g	146.14	8.90E-06	8.90E-05	1.78E-04
Glutaric	4.34	5.3	1400	20	74	108	0.0013g	0.013g	0.026g	132.12	9.84E-06	9.84E-05	1.97E-04
Succinic	4.21	5.65	88	24	82	132	0.0013g	0.013g	0.026g	118.09	1.10E-05	1.10E-04	2.20E-04
NaCl				37	274	524	0.0013g	0.013g	0.026g	58.44	2.22E-05	2.22E-04	4.45E-04

Table II presents the details of contamination amounts at 100 ml deionized water and the concentration equivalent in order to have an equal conductivity level for all contamination types. Three voltages, 5, 7.5, and 10 V at a similar conductivity level for each contamination type, have been studied for this part. It means for the second experimental setup, 12 conditions with ten replications at 3600 min using droplet tests on SMC surfaces have been provided.

TABLE II.

OVERVIEW OF THE SECOND EXPERIMENTAL SETUP USING A SIMILAR CONDUCTIVITY LEVEL.

Contaminations	Amount of contaminations (g) at 100ml D-Water	Contamination levels equivalent in order to have same conductivity level (µg/cm²)
Adipic	0.1131	87
Glutaric	0.0845	65
Succinic	0.0585	45
NaCl	0.00975	7.5

C. Statistical and probabilistic distribution analysis

Statistical analysis is used to extract information from the experimental dataset (descriptive) and use it to discover the behavioural trends (inferential). Probabilistic distribution analysis also integrates information from a dataset to catch the appropriate distributions to calculate the PoF at three periods for each condition. In order to obtain reasonable statistical averages of the LC and specially TTF due to ECM, the droplet test was replicated many times (at least twenty times) to see twenty failures under each experimental condition in the first experimental setup (same contamination levels) and ten replications in the second experimental setup (same conductivity level).

The importance of recognizing the applicable probabilistic distribution for each condition is to endeavour to estimate the average value and uncertainty bound associated with the TTF of SMC to identify and characterise the dataset trend using mathematical formulas. The mathematical formulas for distributions and their graphs give us a better understanding of the dataset and help with quantification for proper comparing

and assessing [28], [29]. In this study, three common continuous probabilistic distributions have been employed, including; Weibull, Lognormal, and Loglogistic distribution. The Loglogistic distribution has a similar shape and follows the same way as the Lognormal distribution obtained from the normal distribution for logistic distribution [30]. These two distributions, with the Weibull distribution as unique distribution due to high flexibility and the most widely used distribution in accelerated failure time, play a central role in the field of risk and reliability analysis [31], [32], [33], [34]. Cumulative distribution function (CDF) for 3-parameter Weibull distribution follows (1) [35], [36], [37];

$$F(t) = 1 - \exp[-\left(\frac{t-\theta}{\alpha}\right)^{\beta}] \qquad (1)$$

In which α is the scale parameter, β is the shape parameter, and θ is the location parameter. The CDF of 3-parameter Lognormal distribution given by (2) [38], [39], [40];

$$F(t) = \Phi(\frac{\ln(t-\gamma)-\mu}{\sigma}) \qquad (2)$$

In which µ is the mean value or scale parameter, σ is the standard deviation or shape parameter, γ is the threshold or location parameter, and Φ is the standard normal distribution. The CDF of 3-parameter Loglogistic distribution is (3) [41], [42];

$$F(t) = [1 + (1 + \frac{\beta}{\sigma}(t-\mu))^{\frac{-1}{\beta}}]^{-1} \qquad (3)$$

In which σ is the scale parameter, β is the shape parameter, and µ is the location parameter.

III. RESULTS AND DISCUSSIONS

An in-situ study on ECM failure mechanism on SMC using droplet test demonstrated the electrochemical failure process, resulting in some evident dendrite formation and the short circuits under various conditions combined with different contamination types/levels and applied voltage. For instance, Fig. 3 illustrates the leak current measurement versus time at one condition combined with 5 µg/cm² adipic acid at 10 V using the potentiostat on an SMC. The ECM grows from the cathode to

the anode during the 160 sec. In these phenomena, the water droplet has electrolyzed at the anode electrode and causes metal ions to dissolve. The metal ions migrate to the cathode through conductive water, which depends on the effective electrical field (E) strength. The Electric field is in relationship with pitch distance (P) and applying potential bias (V) between two electrodes (E=V/P). Ultimately, the metal ions have reduced at the cathode, which relates to the induced contamination type and the level. Then a leak current can emerge on the surface.

Consequently, their deposition at the cathode starts the creation of metallic filaments of dendritic shape in the surface conductive electrolyte. Creating permanent bridging between anode and cathode and leading to malfunctions performance of electronic components and systems owing to the high level of leak current and electric short circuits. In Fig. 3, after 120 sec (TTF), the big jump in leak current presents the creation of a permanent bridge (connection) between two electrodes on the SMC surface. Fig. 4 shows an average of leak current before the big jump (TTF) calculated as LC for each condition. The average of LC values using NaCl contamination compare to WOAs for the same contamination levels, and voltages show very high notable levels; however, the incremental trend from low to high levels of voltage and contamination levels for each contamination type are clearly observable.
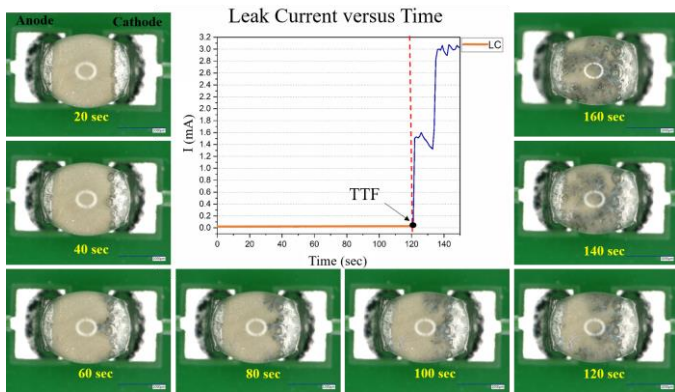

Fig. 3. Leak current measurement versus time with the real picture of dendrite formation and ECM on an SMC under 10 V and 5 µg/cm² adipic acid as contamination type and level.
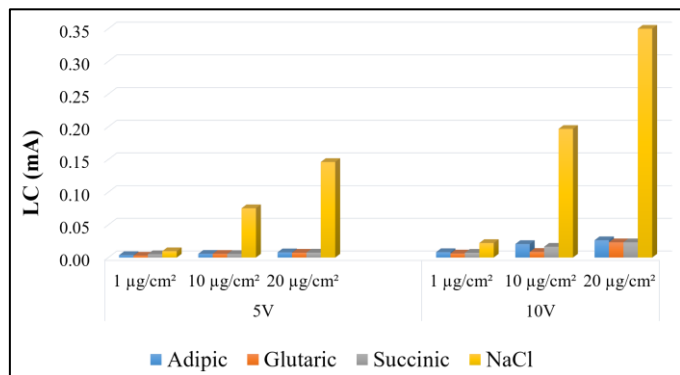

Fig. 4. Comparison of LC averages at various conditions combined of contamination type, levels and applied voltage.

A. TTF in the same contamination levels

In order to investigate contamination types and voltage effects on TTFs at various contamination levels, the first twenty experiments were performed on each condition combined with contamination type, level, and voltage on the same SMC with the specific pitch distance and material. Fig. 5 displays the number of failures at 20 repetitions, as well as the average of TTFs for each condition. The figure shows the lowest number of failures at the low voltage for all contamination types. Moreover, it presents the highest number of failures for low, medium, and high levels of all WOAs, respectively. Increasing the level of contaminations (WOAs) on the chip capacitor surface means reducing the number of components that showed ECM. It might be because of the existing high amount of contamination ions at very narrow spaces between two opposite potential biases of electrodes on the component and works as inhibitors to prevent the growth of dendrite formation and create electrode connections. Nevertheless, NaCl acts opposite to the WOAs.
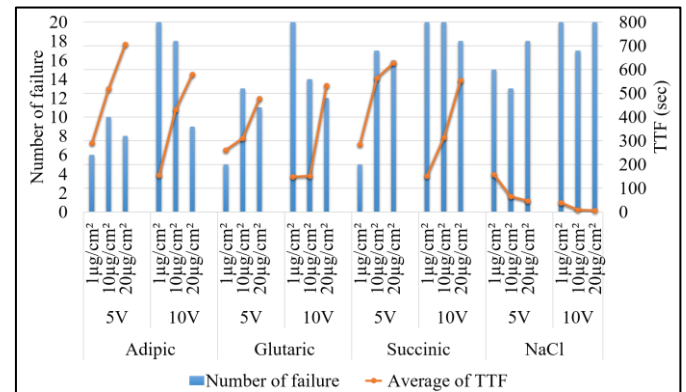

Fig. 5. Number of failures and the average of TTFs at twenty replications for each condition on SMCs.

Fig. 6 shows the typical surface of the chip capacitors views using a digital microscope after the droplet tests. It shows ECM, permanent dendrite filament and corrosion failure on SMC employing the four contamination types and under a similar contamination level (5.5 µg/cm²) and voltage (5 V) with three replications.
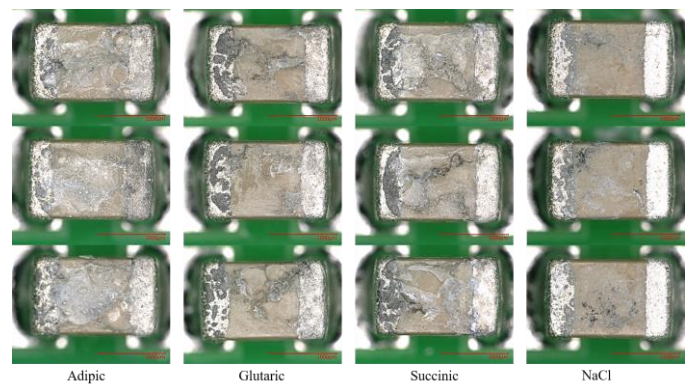

Fig. 6. Optical appearance of dendrite formation and ECM on SMC at four contamination types and the same contamination level (5.5 µg/cm²) and voltage (5 V) with three replications.

Secondly, to make appropriate probabilistic distribution for each condition, we perform more experiments to catch 20 failure

data for each one. According to the comparison of probability plots employing least squares estimation methods by considering twenty TTF values of replications in each condition, applicable probabilistic distributions for each condition according to the Anderson-Darling (AD) value, correlation coefficient, and P-value metrics from the goodness of fit tests have been selected. Generally, with a good approximation, 3-parameter Weibull distribution for all conditions consisting of adipic acid, 3-parameter Lognormal distribution for every condition consisting of succinic acid, and 3-parameter Loglogistic distribution for whole conditions consisting of glutaric acid and NaCl as contamination types, presented appropriate probabilistic distributions according to the value of the metrics. Fig. 8 presents probability plots of entire conditions, which are categorized into four main parts according to the used contamination types. The figure also shows the three parameters (shape/location, scale, Threshold) values of each fitted distribution for every condition, which is based on the CDF according to the specific formula for each distribution calculated and plotted in Fig. 9 to estimate PoF at the desired time.

Table III illustrates the percentage of PoF at three times or periods; i. less than or equal to 300 sec (5 min), ii. less than or equal to 600 sec (10 min), and less than or equal to 900 sec (15 min) according to the CDF and Fig. 9. The percentage PoF for each condition in this table presents the likelihood or chance of a big jump in leak current and generating ECM and dendrite formation based on the combination of different contamination types/levels and voltages. The last coloured column has been brought to quickly compared the effect of contamination types and voltage at the same contamination levels. Fig. 7 demonstrates the conductivity levels of all contamination solutions at three levels. The NaCl conductivity at the same contamination levels presents the highest values compared to WOAs. However, the conductivity levels of WOAs with adipic, glutaric, and succinic arrangements are close to each other from low to high values. Due to the different conductivity levels of contamination types at the same contamination levels and in relation to Fig. 5, the number of failures at twenty replication follows the same order, and the succinic acid presents the highest number of failures camper to other WOAs.

TABLE III.
PoF AT THREE DIFFERENT TIMES/PERIODS FOR EACH CONDITION.

Condition	Aplicable Distribution	PoF (%)			
		≤ 5 min	≤ 10 min	≤ 15 min	Average
Adipic, 1µg/cm², 5V	Weibull (3P)	65.6	99.58	99.99	88.39
Adipic, 10µg/cm², 5V		0	81.83	99.98	60.60
Adipic, 20µg/cm², 5V		4.77	24.59	80.24	36.53
Adipic, 1µg/cm², 10V		97.65	99.99	100	99.21
Adipic, 10µg/cm², 10V		4.8	99.72	100	68.17
Adipic, 20µg/cm², 10V		10.75	52.06	92.81	51.87
Glutaric, 1µg/cm², 5V	Loglogistic (3P)	99.99	100	100	100.00
Glutaric, 10µg/cm², 5V		61.12	89.79	95.47	82.13
Glutaric, 20µg/cm², 5V		44.85	70.64	81.18	65.56
Glutaric, 1µg/cm², 10V		98.18	99.98	99.99	99.38
Glutaric, 10µg/cm², 10V		97.17	99.74	99.93	98.95
Glutaric, 20µg/cm², 10V		15.09	50.81	85.61	50.50
Succinic, 1µg/cm², 5V	Lognormal (3P)	63.67	99.4	99.99	87.69
Succinic, 10µg/cm², 5V		4.21	49.53	95.52	49.75
Succinic, 20µg/cm², 5V		2.39	46.86	91.5	46.92
Succinic, 1µg/cm², 10V		97.18	99.93	99.99	99.03
Succinic, 10µg/cm², 10V		52.4	96.62	99.82	82.95
Succinic, 20µg/cm², 10V		11.73	65.78	90.27	55.93
NaCl, 1µg/cm², 5V	Loglogistic (3P)	92.09	98.36	99.33	96.59
NaCl, 10µg/cm², 5V		99.44	99.92	99.98	99.78
NaCl, 20µg/cm², 5V		97.88	99.19	99.54	98.87
NaCl, 1µg/cm², 10V		99.96	99.99	99.99	99.98
NaCl, 10µg/cm², 10V		97.92	98.68	98.98	98.53
NaCl, 20µg/cm², 10V		100	100	100	100.00

Generally, the average of PoFs for all conditions in 10 V were higher than the same conditions in 5 V, which is proportional to LCs levels displayed in Fig. 4, and the inverse of the number of failures plotted at each condition according toFig. 5 The importance of the high voltage in relation to TTF in the same contamination type/level, and constant other influence factors such as temperature (at ambient temperature), and pitch distance (on the same SMC surface), because of the extent of electrical field and the leak current, that can be passed through the droplet solutions. Therefore, an increase in voltage will influence the leak current and start faster metal ions dissolution and dendrite formation on the SMC surface, subsequently creating the PoF in the early times.
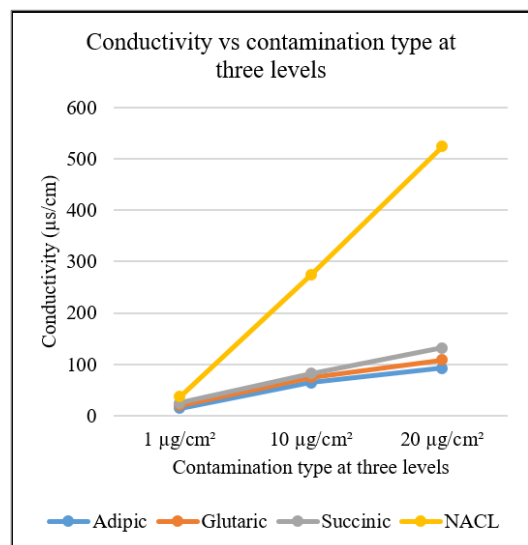

Fig. 7. Conductivity plot at various contamination types/levels.

Presented at the Nordic Microelectronics and Packaging Conference and Exhibition (NordPac) 2023   5
Authorized licensed use limited to: Danmarks Tekniske Informationscenter. Downloaded on July 25,2023 at 09:02:11 UTC from IEEE Xplore. Restrictions apply.
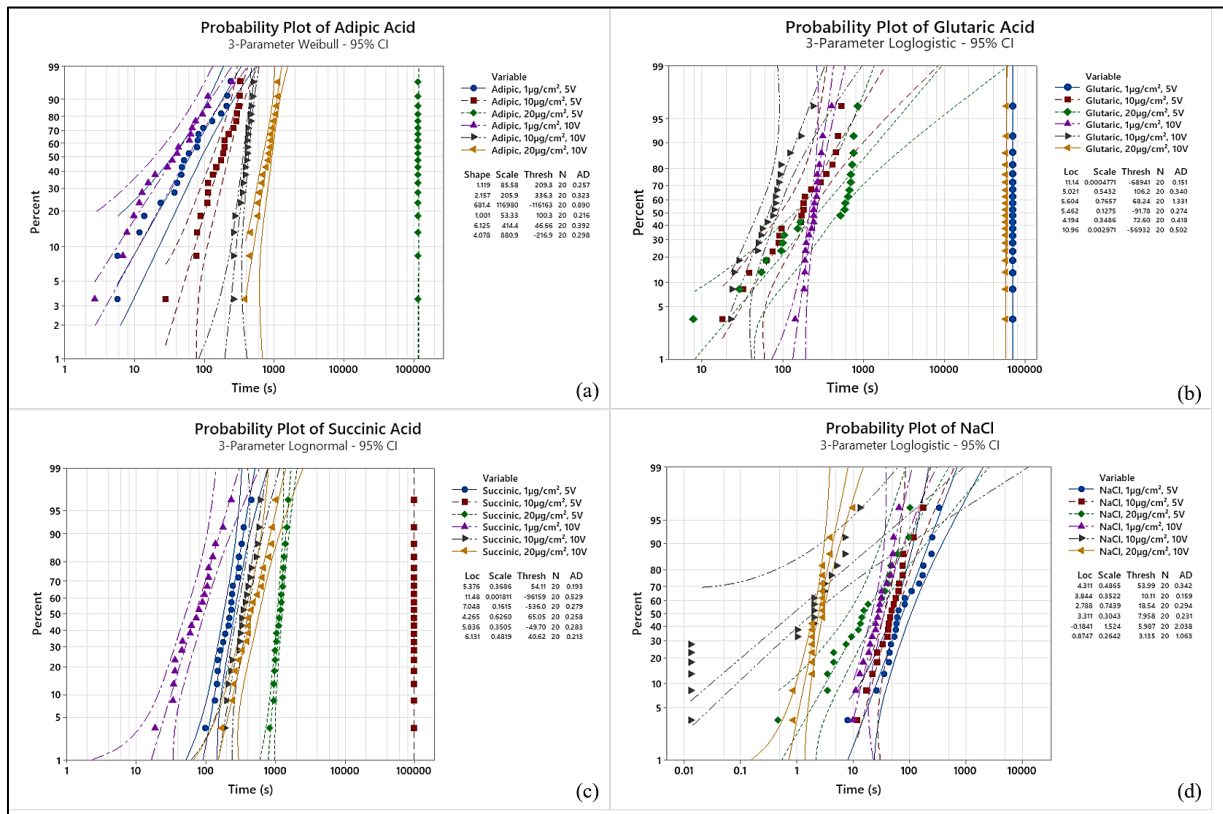
Fig. 8. Probability plots of various conditions are categorized into four main parts according to the contamination types used.
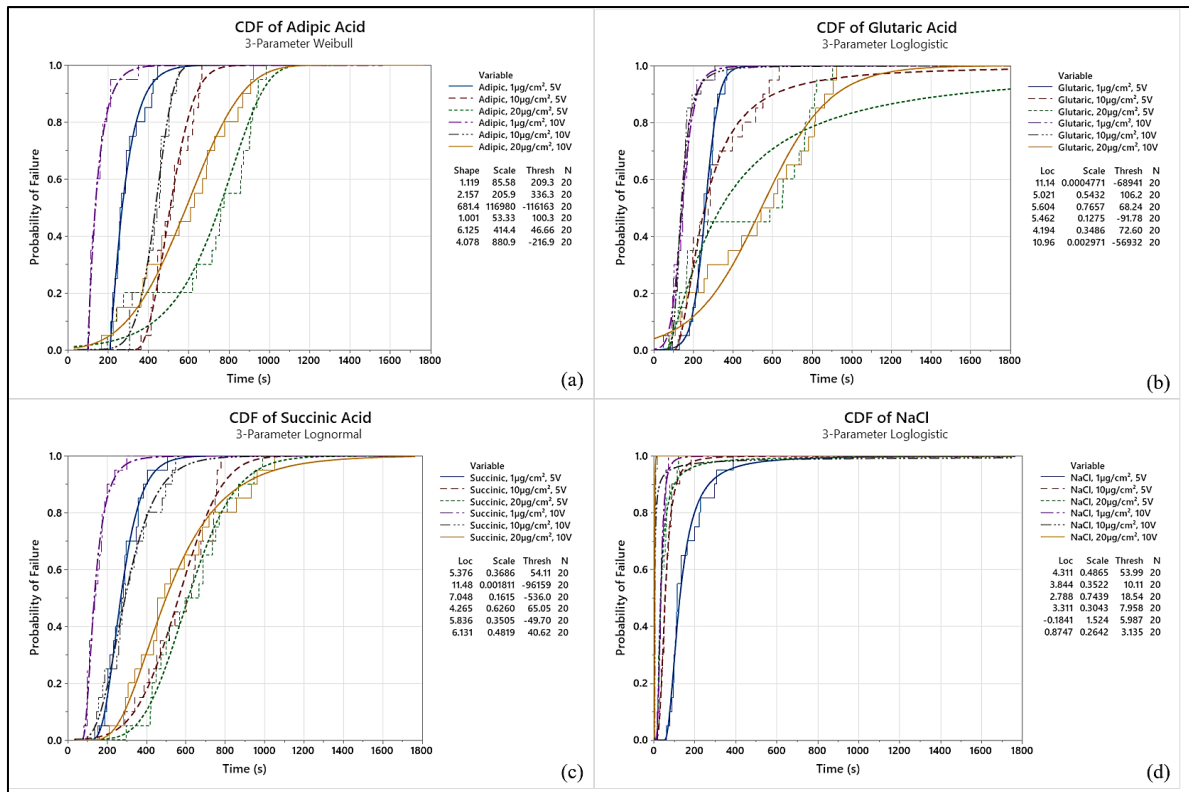

Fig. 9. CDF plots of various conditions that categorized into four parts based on contamination types.

In addition, the average of PoF for all WOAs at both voltages shows a decreasing trend from low to high contamination levels. However, the PoF for NaCl offers an increasing trend from low to high levels of contamination. It might be because of the deposit of the high amount of contamination ions at spaces between two electrodes, which works as inhibitors to prevent the growth of dendrite formation and create failure. Fig. 10 presents the average PoF of various contamination types at the same contamination levels for the three times/periods 300 sec, 600 sec, and 900 sec. Moreover, from all of the contaminations, NaCl demonstrates the highest average of PoF at the same contamination levels. Glutaric acid after NaCl presents the highest average of PoF at WOAs due to having a highly aggressive conductivity camper to other WOAs. The average percentage of PoF for succinic and adipic acid approximately are the same with little difference, showing that succinic acid's more aggressive.
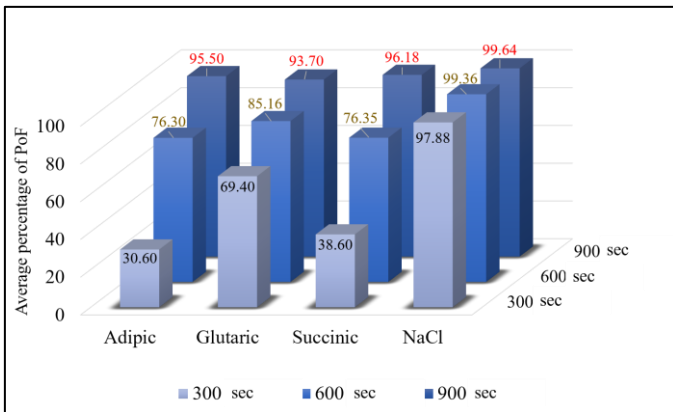

Fig. 10. Average percentage of PoF of various contamination types at the same contamination levels for three times/periods 5, 10, and 15 min.

B. TTF in similar conductivity

To understand the effect of contamination type and voltage on TTF under the same conductivity value, 12 new experiments have been performed using new solutions for all contamination types, according to Table 2 information. Using the solutions with equal conductivity levels and the droplet test, the same value (2 µl) as the first experimental setup in ten replications have performed on the SMC. Fig. 11 illustrates the statistical TTF values of the experimental dataset on the same conductivity value and different contamination types and voltages. This figure shows that in the same conductivity levels of each contamination solution, besides similar voltages, the TTF level of NaCl is significantly lesser than WOAs. It means the period to create ECM and failure employing NaCl even in the same conductivity levels is still lower than other WOAs contamination. The remarkable results of this part present the significant effect of succinic acid on SMC TTF, which is higher than glutaric and adipic acid, respectively, which offer a lower average of TTF comper to specially glutaric and adipic acid in these conditions.
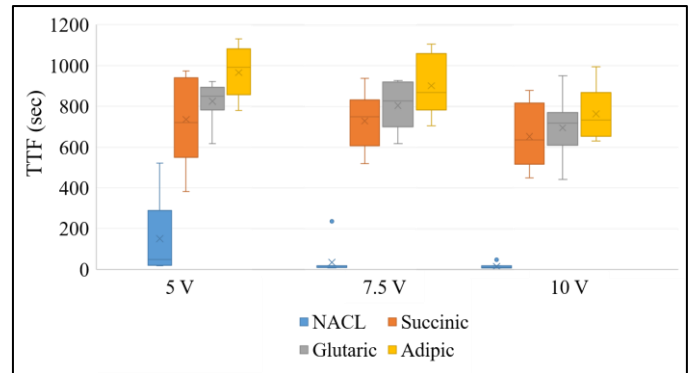

Fig. 11. Box diagram of experimental data TTFs on the same conductivity value and different contamination types and voltages.

Fig. 12. presents the comparison of the average TTF and failure rate of contaminations at three voltages and the same conductivity level. Failure rate refers to the failure speed and is calculated by the number of failures divided by the total operation time. The failure rate was calculated by dividing the number of SMC failures per 18000 sec (10 samples for each condition* 30 minutes for each run* 60 seconds for each min) in the unit of s^{-1}. The red column illustrates the average failure rate at three voltages and the same conductivity level for four contaminations. The results show that succinic acid in the same conductivity level gives a higher average failure rate. This refers to the high number of SMC failures for using succinic acid at the same conditions comper to other WOAs and even the NaCl. Moreover, in the same conductivity level, the TTF at each contamination type from low to high voltage levels illustrate the descending trend.

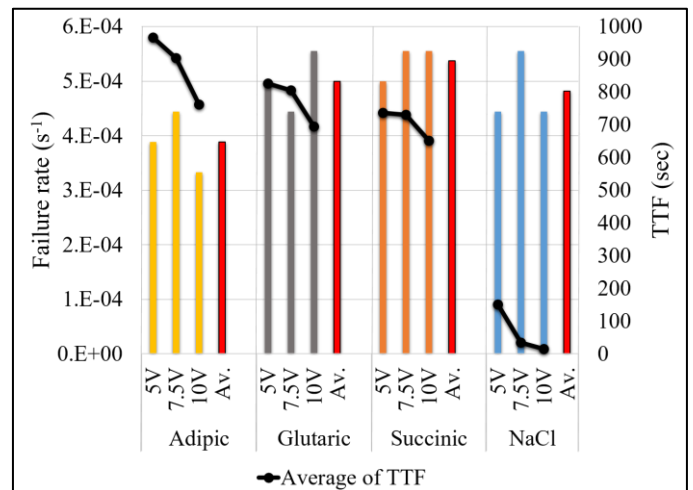Fig. 12. Comparison of the average TTF and failure rate of contaminations at the same conductivity level.

IV. CONCLUSIONS

• Droplet test results investigation showed that the mostly TTF values increased with increasing the contamination levels and decreasing voltage levels in all WOAs. However, the number of failures and PoF increased with increasing the voltage and decreasing the contamination levels in all WOAs. With only

NaCl, TTF decreased, and the number of failures increased with increasing the contamination levels and voltage levels..

• In the same contamination level at whole contamination types, from the low level to the high level of voltage, TTF decreased, and the number of failures increased. Except for NaCl, at a similar voltage level, the lower contamination level has the lowest average of TTF.

• Generally, the average of TTF from all contamination levels at the high voltage level is always lower than the low voltage level for all contaminations. However, the average number of failures at the high voltage level is usually higher than at the low voltage level.

• Generally, in the same contamination level (or the same amount of contamination solved in 100 ml distilled water) at whole contamination types, conductivity and the number of failures follow the same order as; NaCl>Succinic>Glutaric>Adipic, and the average of TTF follows the order as; NaCl<Glutaric<Succinic<Adipic. (Due to existing glutaric acid results, we could not wholly say that conductivity has an inverse relation with TTF).

• In the equal conductivity level, the average TTF with increasing voltage levels decreased and followed the order as; NaCl<Succinic<Glutaric<Adipic.

• The average failure rate in the same conductivity level shows NaCl has the lowest value. Moreover, after that, succinic, glutaric, and adipic acid present the lowest failure rate, respectively.

REFERENCES

[1] S. Zhan, M. H. Azarian, and M. Pecht, "Reliability of Printed Circuit Boards Processed Using No-Clean Flux Technology in Temperature–Humidity–Bias Conditions," *IEEE Trans. Device Mater. Reliab.*, vol. 8, no. 2, pp. 426–434, Jun. 2008, doi: 10.1109/TDMR.2008.922908.

[2] V. Verdingovas, S. Joshy, M. S. Jellesen, and R. Ambat, "Analysis of surface insulation resistance related failures in electronics by circuit simulation," *Circuit World*, vol. 43, no. 2, pp. 45–55, May 2017, doi: 10.1108/CW-09-2016-0040.

[3] K. S. Hansen, M. S. Jellesen, P. Moller, P. J. S. Westermann, and R. Ambat, "Effect of solder flux residues on corrosion of electronics," in *2009 Annual Reliability and Maintainability Symposium*, Jan. 2009, pp. 502–508, doi: 10.1109/RAMS.2009.4914727.

[4] V. Verdingovas, M. S. Jellesen, and R. Ambat, "Relative effect of solder flux chemistry on the humidity related failures in electronics," *Solder. Surf. Mt. Technol.*, vol. 27, no. 4, pp. 146–156, Sep. 2015, doi: 10.1108/SSMT-11-2014-0022.

[5] S. Zhan, M. H. Azarian, and M. G. Pecht, "Surface insulation resistance of conformally coated printed circuit boards processed with no-clean flux," *IEEE Trans. Electron. Packag. Manuf.*, vol. 29, no. 3, pp. 217–223, Jul. 2006, doi: 10.1109/TEPM.2006.882496.

[6] S. Bahrebar and R. Ambat, "Time to Failure Prediction on a Printed Circuit Board Surface Under Humidity Using Probabilistic Analysis," *J. Electron. Mater.*, vol. 51, no. 8, pp. 4388–4406, Aug. 2022, doi: 10.1007/s11664-022-09668-7.

[7] S. Bahrebar, "Climatic Reliability of Electronics: Prediction of PCB Failure under Humidity using Predictive Analytics," Technical University of Denmark (DTU), 2022.

[8] R. Ambat and K. Piotrowska, "Importance of PCBA cleanliness in humidity interaction with electronics," in *Humidity and Electronics*, Elsevier, 2022, pp. 141–196.

[9] V. Verdingovas, M. S. Jellesen, and R. Ambat, "Impact of NaCl contamination and climatic conditions on the reliability of printed circuit board assemblies," *IEEE Trans. Device Mater. Reliab.*, vol. 14, no. 1, pp. 42–51, 2014, doi: 10.1109/TDMR.2013.2293792.

[10] V. Verdingovas, M. S. Jellesen, and R. Ambat, "Solder Flux Residues and Humidity-Related Failures in Electronics: Relative Effects of Weak Organic Acids Used in No-Clean Flux Systems," *J. Electron. Mater.*, vol. 44, no. 4, pp. 1116–1127, Apr. 2015, doi: 10.1007/s11664-014-3609-0.

[11] K. Piotrowska and R. Ambat, "Residue-Assisted Water Layer Build-Up Under Transient Climatic Conditions and Failure Occurrences in Electronics," *IEEE Trans. Components, Packag. Manuf. Technol.*, vol. 10, no. 10, pp. 1617–1635, Oct. 2020, doi: 10.1109/TCPMT.2020.3005933.

[12] M. S. Jellesen, P. Westermann, V. Verdingovas, P. Holm, and R. Ambat, "Relation Between PCBA Cleanliness and Climatic Reliability," 2011.

[13] S. Bahrebar, S. Homayoun, and R. Ambat, "Using Machine Learning Algorithms to Predict Failure on the PCB Surface under Corrosive Conditions," *Corros. Sci.*, p. 110500, Jul. 2022, doi: 10.1016/J.CORSCI.2022.110500.

[14] S. Bahrebar and R. Ambat, "Investigation of critical factors effect to predict leakage current and time to failure due to ECM on PCB under humidity," *Microelectron. Reliab.*, vol. 127, p. 114418, Dec. 2021, doi: 10.1016/j.microrel.2021.114418.

[15] J. J. Steppan, J. A. Roth, L. C. Hall, D. A. Jeannotte, and S. P. Carbone, "A Review of Corrosion Failure Mechanisms during Accelerated Tests: Electrolytic Metal Migration," *J. Electrochem. Soc.*, vol. 134, no. 1, pp. 175–190, Jan. 1987, doi: 10.1149/1.2100401.

[16] K. Piotrowska, F. Li, and R. Ambat, "Thermal decomposition of binary mixtures of organic activators used in no-clean fluxes and impact on PCBA corrosion reliability," *Solder. Surf. Mt. Technol.*, vol. 32, no. 2, pp. 93–103, Aug. 2019, doi: 10.1108/SSMT-05-2019-0020.

[17] K. Piotrowska, R. Ud Din, F. B. Grumsen, M. S. Jellesen, and R. Ambat, "Parametric Study of Solder Flux Hygroscopicity: Impact of Weak Organic Acids on Water Layer Formation and Corrosion of Electronics," *J. Electron. Mater.*, vol. 47, no. 7, pp. 4190–4207, 2018, doi: 10.1007/s11664-018-6311-9.

[18] K. Piotrowska, V. Verdingovas, and R. Ambat, "Humidity-related failures in electronics: effect of binary mixtures of weak organic acid

activators," *J. Mater. Sci. Mater. Electron.*, vol. 29, no. 20, pp. 17834–17852, Oct. 2018, doi: 10.1007/s10854-018-9896-0.

[19] K. Piotrowska, M. Grzelak, and R. Ambat, "No-Clean Solder Flux Chemistry and Temperature Effects on Humidity-Related Reliability of Electronics," *J. Electron. Mater.*, vol. 48, no. 2, pp. 1207–1222, Feb. 2019, doi: 10.1007/s11664-018-06862-4.

[20] B. Cao, Q. Tang, and G. Cheng, "Recent advances of zwitterionic carboxybetaine materials and their derivatives," *J. Biomater. Sci. Polym. Ed.*, vol. 25, no. 14–15, pp. 1502–1513, Oct. 2014, doi: 10.1080/09205063.2014.927300.

[21] Y. Wang *et al.*, "Enhanced PCBs sorption on biochars as affected by environmental factors: Humic acid and metal cations," *Environ. Pollut.*, vol. 172, pp. 86–93, Jan. 2013, doi: 10.1016/j.envpol.2012.08.007.

[22] V. Verdingovas, M. S. Jellesen, and R. Ambat, "Influence of sodium chloride and weak organic acids (flux residues) on electrochemical migration of tin on surface mount chip components," *Corros. Eng. Sci. Technol.*, vol. 48, no. 6, pp. 426–435, Sep. 2013, doi: 10.1179/1743278213Y.0000000078.

[23] D. Minzari, "Investigation of Electronic Corrosion Mechanisms," Technical University of Denmark, 2010.

[24] D. Minzari, M. S. Jellesen, P. Møller, and R. Ambat, "On the electrochemical migration mechanism of tin in electronics," *Corros. Sci.*, vol. 53, no. 10, pp. 3366–3379, Oct. 2011, doi: 10.1016/J.CORSCI.2011.06.015.

[25] H. Conseil-Gudla, M. S. Jellesen, and R. Ambat, "Printed Circuit Board Surface Finish and Effects of Chloride Contamination, Electric Field, and Humidity on Corrosion Reliability," *J. Electron. Mater.*, vol. 46, no. 2, pp. 817–825, Feb. 2017, doi: 10.1007/s11664-016-4974-7.

[26] K. Piotrowska, "Water film formation on PCBA surface - Investigation of aspects contributing to premature corrosion failures and safety measures for electronics reliability improvement," Technical University of Denmark, 2018.

[27] A. Apelblat and E. Manzurola, "Solubility of oxalic, malonic, succinic, adipic, maleic, malic, citric, and tartaric acids in water from 278.15 to 338.15 K," *J. Chem. Thermodyn.*, vol. 19, no. 3, pp. 317–320, Mar. 1987, doi: 10.1016/0021-9614(87)90139-X.

[28] S. Bahrebar, D. Zhou, S. Rastayesh, H. Wang, and F. Blaabjerg, "Reliability assessment of power conditioner considering maintenance in a PEM fuel cell system," *Microelectron. Reliab.*, vol. 88–90, no. September, pp. 1177–1182, 2018, doi: 10.1016/j.microrel.2018.07.085.

[29] P. V. Varde and M. G. Pecht, "Probabilistic approach to reliability engineering," in *Springer Series in Reliability Engineering*, vol. 0, no. 9789811300882, 2018.

[30] V. P. Singh, H. Guo, and F. X. Yu, "Parameter estimation for 3-parameter log-logistic distribution (LLD3) by Pome," *Stoch. Hydrol. Hydraul.*, vol. 7, no. 3, pp. 163–177, Sep. 1993, doi: 10.1007/BF01585596.

[31] S. T. Okpala and Okoli, "Comparison on performance of the lognormal, log logistic and weibull distribution on survival of hiv patients with opportunistic infections in anambra state, nigeria," *Eur. J. Stat. Probab.*, vol. 8, no. 2, pp. 14–24, 2020.

[32] S. Eze, "Comparison on performance of the Lognormal, Log logistic and Weibull Distribution on Survival of HIV Patients," *https://www.eajournals.org/*, Sep. 2020.

[33] J. S. Kim and B.-J. Yum, "Selection between Weibull and lognormal distributions: A comparative simulation study," *Comput. Stat. Data Anal.*, vol. 53, no. 2, pp. 477–485, Dec. 2008, doi: 10.1016/j.csda.2008.08.012.

[34] S. Bahrebar, S. Rastayesh, K. Sepanloo "Dynamic Availability Assessment on Tehran Research Reactor Water Brief Description of TRR Cooling," *Indian J.Sci.Res.*, vol. 1, no. 2, pp. 471–474, 2014.

[35] O. Osarumwense and N. C. Rose, "Parameters estimation methods of the Weibull distribution : A comparative study," *Elixir Stat. 69*, vol. 69, no. April 2014, pp. 23177–23184, 2014.

[36] M. Alqam, R. M. Bennett, and A.-H. Zureick, "Three-parameter vs. two-parameter Weibull distribution for pultruded composite material properties," *Compos. Struct.*, vol. 58, no. 4, pp. 497–503, Dec. 2002, doi: 10.1016/S0263-8223(02)00158-7.

[37] G. C. A. Tolentino, J. V. Leite, M. Rossi, O. Ninet, G. Parent, and J. Blaszkowski, "Modeling of Magnetic Anisotropy in Electrical Steel Sheet by Means of Cumulative Distribution Functions of Gaussians," *IEEE Trans. Magn.*, vol. 58, no. 8, pp. 1–5, Aug. 2022, doi: 10.1109/TMAG.2022.3166117.

[38] R. J. Aristizabal, "Estimating the Parameters of the Three-Parameter Lognormal Distribution," Florida International University, 2012.

[39] C. Chatfield, N. L. Johnson, S. Kotz, and N. Balakrishnan, "Continuous Univariate Distributions," *Stat.*, vol. 44, no. 4, p. 544, 1995, doi: 10.2307/2348907.

[40] T. M. M. Farley and W. Nelson, "Applied Life Data Analysis.," *Biometrics*, vol. 39, no. 3, p. 820, Sep. 1983, doi: 10.2307/2531130.

[41] M. El Genidy, D. Abd, E.-S. Abd El-Rahman, M. Mohammed, and E. Genidy, "Three Parameters Estimation of Log-Logistic Distribution Using Algorithm of Percentile Roots," *54th Annu. Conf. Stat. Comput. Sci. Oper. Res.*, vol. 9, pp. 9–11, 2019.

[42] B. A. Para, T. R. Jan, and M. Subzar, "A New Three Parameter Log-Logistic Model for Survival Data Analysis," *J. Stat. Appl. Probab.*, vol. 10, no. 3, pp. 705–714, Nov. 2021, doi: 10.18576/jsap/100310.